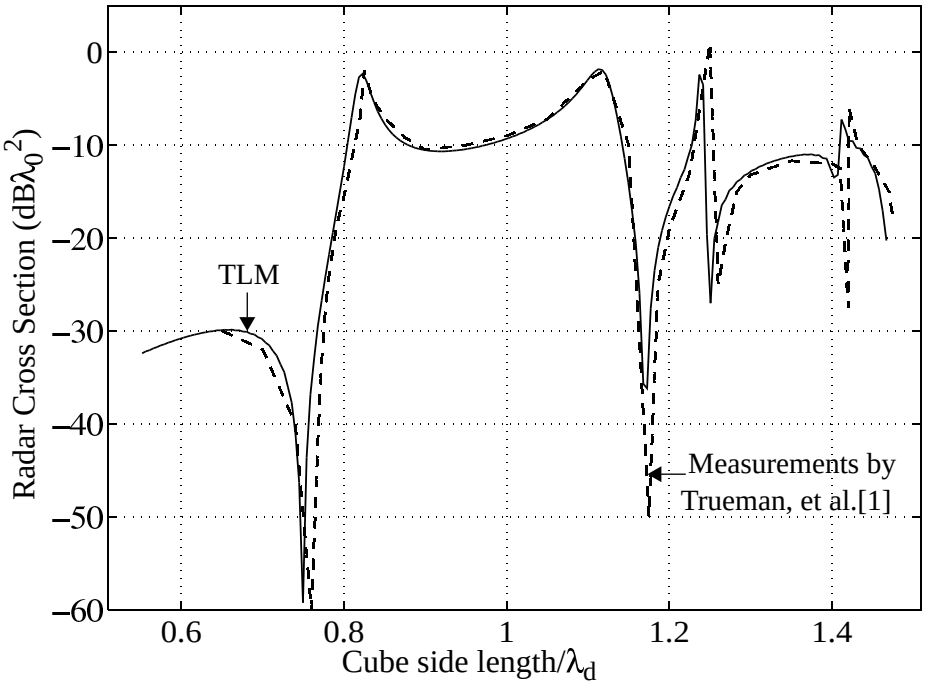

Fig. 6: RCS computed with 60,000 TLM time steps (cube side length = 8.97 mm, ε_r = 37.84, bistatic angle = 8 degrees)

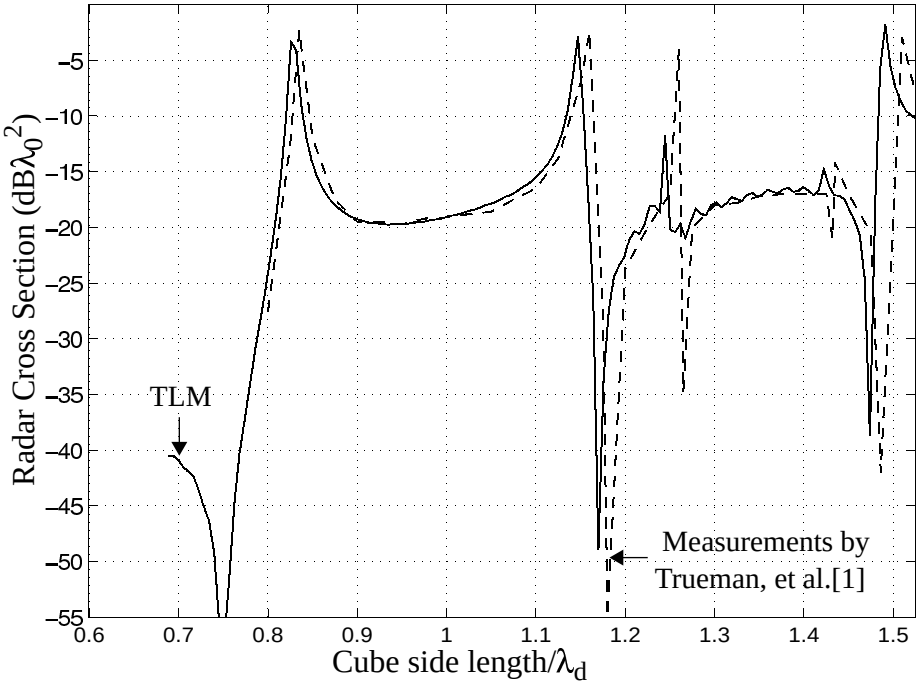

Fig. 7: RCS computed with 60,000 TLM time steps (cube side length = 7.72 mm, ε_r = 79.46, bistatic angle = 8 degrees)

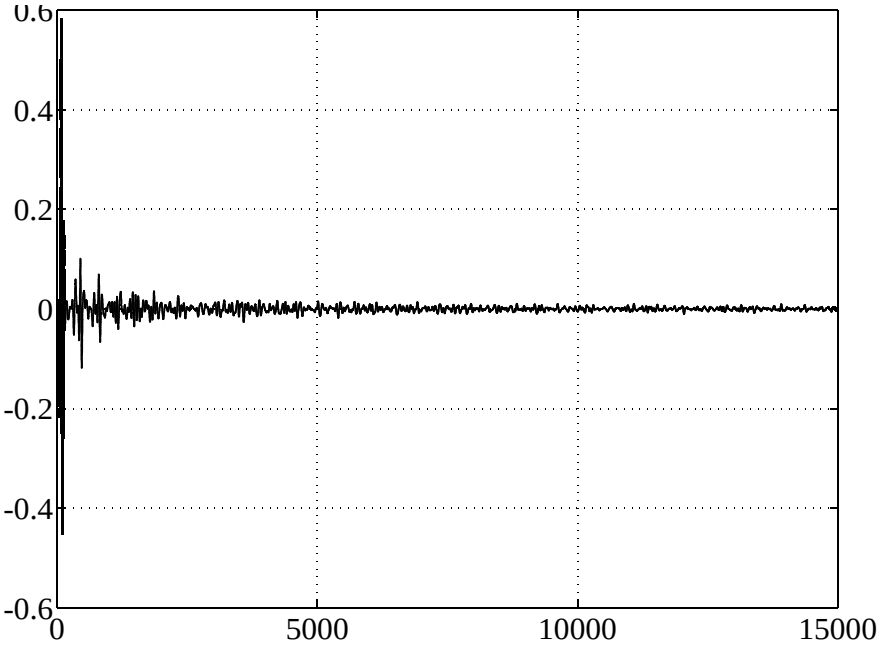

Fig. 4b: Time response of the high permittivity cube for a=b= - 0.25 (ε_r=37.84, θ_1=45 ^{0}, θ_2=85^0)

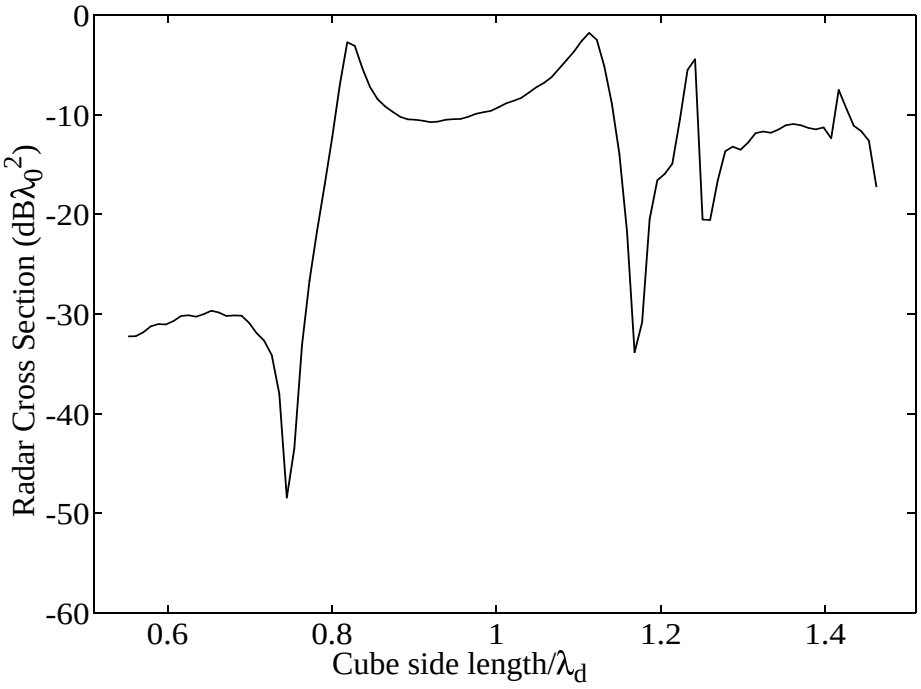

Fig. 5: RCS computed with 15,000 TLM time steps (cube side length = 8.97 mm, ε_r = 37.84, bistatic angle = 8 degrees)

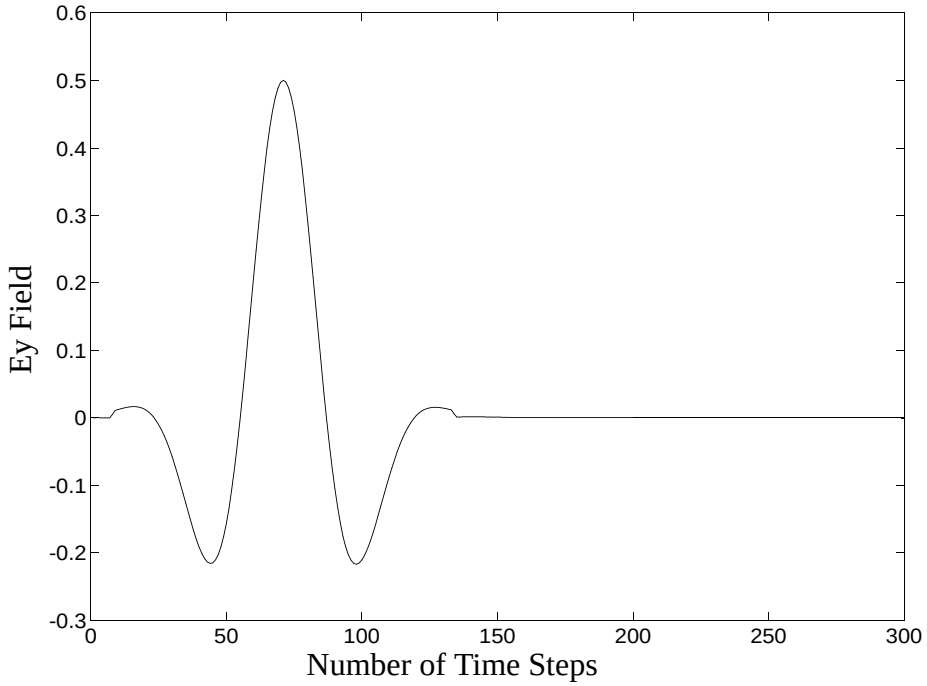

Fig. 3: Cosine modulated Gaussian temporal profile for the plane wave excitation

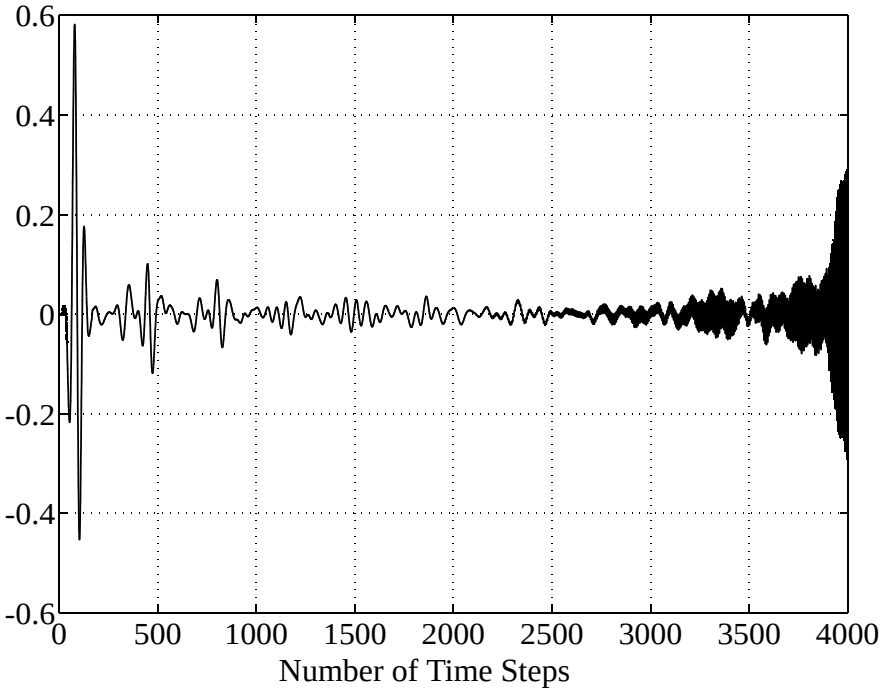

Fig. 4a: Time response of the high permittivity cube for a=b=0.25 (ε_r=37.84, θ_1=45 ^{0}, θ_2=85^0)

100 Mbytes for 100 frequency points). One way of avoiding this is to compute the far -fields directly in the time domain as done in [12]. In that case, Prony's method can be applied to estimate the future time response from a short initial time response, leading to a very fast TLM analysis. Our future work will concentrate on these techniques.

REFERENCES

[1] C.W. Trueman, S.J. Kubina, R.J. Luebbers, S.R. Mishra, and C. Larose, "RCS of High Permittivity Cubes by FDTD and by Measurement", *9th Annual Review of Progress in Applied Computational Electromagnetics* Digest, pp. 2-10, March 22-26, 1993, Monterey, CA.

[2] W. J. R. Hoefer, "The Transmission Line Matrix (TLM) Method", in T. Itoh: *Numerical Techniques for Microwave and Millimeter Wave Passive Structures*, John Wiley & Sons, New York (1989).

[3] F.J. German, G.K. Ghothard, L.S. Riggs, and P.M. Goggan, "The Calculation of Radar Cross-section (RCS) Using the TLM Method", Int. J. Numer. Modelling, vol. 2, no. 4, pp. 267-278, Dec. 1989.

[4] N.R.S. Simons and E. Bridges, "Application of the TLM Method to Two-Dimensional Scattering Problems", Int. J. Numer. Modelling, vol. 5, pp. 93-110, 1992.

[5] M. Khalladi, J.A. Morente, and J.A. Porti, "RCS of Arbitrarily-Shaped Targets with the TLM Method", *IEEE Trans. on Antennas and Propagation*, vol. 42, no. 6, pp.891-893, June 1994.

[6] F.J. German, "General Electromagnetic Scattering Analysis by TLM Method", Electronics Letters, vol. 30, no. 9, pp. 689-690, 28th April 1994.

[7] R. L. Higdon, "Numerical absorbing boundary condition for the wave equation," *Mathematics of Computation*, vol. 49, no. 179, pp. 65-91, July 1987.

[8] D. Steich and R. Luebbers, "Comparison and Generation of Higher Order FDTD Absorbing Boundaries", *10th Annual Review of Progress in Applied Computational Electromagnetics* Digest, pp. 212-233, March 21-26, 1994, Monterey, CA.

[9] C. Eswarappa and W.J.R. Hoefer, "One-Way Equation Absorbing Boundary Conditions for 3-D TLM Analysis of Planar and Quasi-planar Structures", *IEEE Trans. Microwave Theory Techniques*, vol. 42, no. 9, pp. 1669-1677, Sep. 1994.

[10] Z. Chen, M.M. Ney, and W.J.R. Hoefer, "Absorbing and Connecting Boundary Conditions for the TLM Method", *EEE Trans. Microwave Theory Tech.*, vol. MTT-41, no. 11, pp. 2016-2024, 1993.

[11] P. B. Johns, "Symmetrical Condensed Node for the TLM method", *IEEE Trans. Microwave Theory Tech.*, vol. MTT-35, no. 4, pp. 370-377, April 1987.

[12] R.J. Luebbers, K.S. Kunz, M. Schneider and F. Hunsberger, "A Finite-Difference Time-Domain Near Zone to Far Zone Transformation", *IEEE Trans. on Antennas and Propagation*, vol. AP-39, No. 4, pp. 429-433, April 1991.

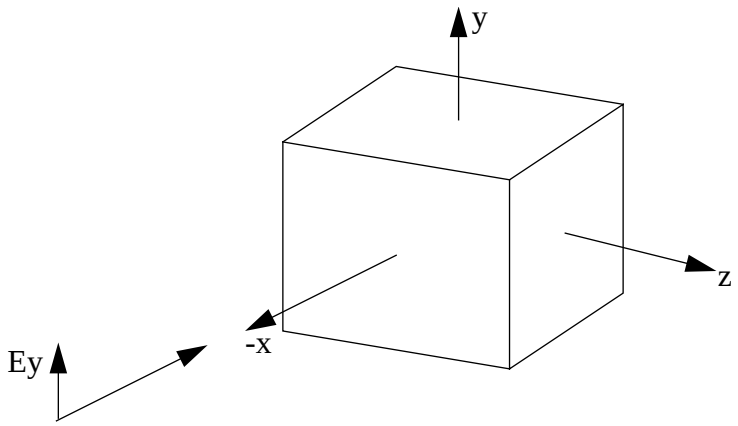

Fig. 2: The high permittivity cube with incident electric field E_y

(weighted time average of the space difference) and *b* (weighted space average of the time difference) are plotted in Figs. 4a and 4b. Note that the oscillations start around 2500 time steps for the case *a*=*b*=0.25, while there is no stability problem for *a*=*b*=-0.25. Hence, we have used *a*=*b*=-0.25 in all our computations. Stability beyond 60,000 time steps has been obtained in both dielectric cubes of permittivity 37.84 and 79.46 with just 20 cells separating the cube edges and the absorbing boundaries, while growing oscillations beyond 32,768 time steps have been reported in the FDTD analysis of the cube of permittivity 79.46 using Mur 's absorbing boundaries (in spite of twice the spacing of 40 cells between the cube edges and the absorbing boundaries).

The computed RCS for 15,000 TLM time steps is plotted in Fig. 5. When compared with the measured results (Fig. 6), it can be seen that the convergence is not yet reached. Fig. 6 shows the RCS data computed with 60,000 time steps. They compare well with the measurements.

Next, we have computed the RCS of a cube of size 7.72 mm and ε_r=79.46 [1]. Again, the same TLM discretization as above (i.e., 15 cells along the length of the cube and 20 cells between the cube edge and the absorbing boundaries) was used. The space resolution and time step were 0.5147 mm and 0.8578 ps, respectively . The width of the cosine modulated Gaussian pulse was 148 Δt. Fig. 7 compares the computed RCS (using 60,000 TLM time steps) and measurement. They compare well except for a slight shift in the TLM results towards lower frequencies because of the coarseness error.

5. CONCLUSIONS

The RCS of high permittivity dielectric cubes has been obtained using the TLM method. The results agree very well with the measurements published in [1]. While the frequency shift between the TLM results and the measurements is negligible for ε_r=37.84, it is very small in the case of ε_r=79.46. A much larger shift has been reported in the FDTD analysis.

Our study shows that Higdon's absorbing boundaries have superior absorption and long term stability. Also, they are very efficient since they need to be placed only 20 cells away from the cube surfaces.

The frequency domain near-field to far-field transformation technique requires huge disk space to store the tangential electric and magnetic f ields on the fictitious current surfaces (of the order of

The values of *a* and *b* can be chosen to control the stability of the absorbing boundaries. According to Higdon [7], *a* must be less than or equal to 0.5 (for *a=b*) to get stable absorbing boundary conditions.

3. NEAR-FIELD TO FAR-FIELD TRANSFORMATION

The near-field to far-field transformation technique based on the equivalence principle is well known. According to this principle, the far electromagnetic field components can be computed if the tangential electric and magnetic fields on a closed fictitious surface surrounding the scatterer are known. If the fields outside of the closed surface are E_s and H_s, then the surface electric and magnetic current densities are

$$J_s = \hat{n} \times H_s, \qquad M_s = -\hat{n} \times E_s, \tag{4}$$

where is the local surface unit normal. These current densities can be calculated using the TLM method. These should be calculated at the required number of frequencies and stored for further processing. After the current densities have been computed, the electric and magnetic vector potentials can be calculated from the following equations:

$$= \frac{\mu e^{-jkr}}{4\pi r} \int_s J_s e^{jk(x_s \sin\theta\cos\phi + y_s \sin\theta\sin\phi + z_s \cos\theta)}\, ds \tag{5}$$

$$= \frac{\varepsilon e^{-jkr}}{4\pi r} \int_s M_s e^{jk(x_s \sin\theta\cos\phi + y_s \sin\theta\sin\phi + z_s \cos\theta)}\, ds \tag{6}$$

where x_s, y_s, and z_s are the co-ordinates of the source point on the current surface. θ and ϕ are the spherical co-ordinates of the far point. The far-field electric components can be computed from the knowledge of electric and magnetic vector potentials:

$$_\theta = -j\omega(A_\theta + \eta F_\phi), \quad E_\phi = -j\omega(A_\phi - \eta F_\theta), \tag{7}$$

where η is the free space impedance.

4. NUMERICAL RESULTS

The dielectric cube of size 8.97 mm and permittivity 37.84 was discretized into 15 SCN-TLM cells on each side. The space resolution and time step were 0.598 mm and 0.9966 ps, respectively. A plane wave with a electric field component E_y and magnetic field component H_z was incident on one face of the cube normally (shown in Fig. 2). This was achieved in the symmetrical condensed node by launching the impulses on branch 3. We have used a cosine modulated Gaussian pulse (shown in Fig. 3) as the excitation to make sure that only the frequencies of interest were excited. This also ensured that the D.C. and very low frequencies were not excited, otherwise, the absorbing boundaries could not be placed close to the cube surface. The excitation Gaussian pulse width (corresponding to -34 dB) was 127 Δt. The values of the incidence angles used in the design of the absorbing boundaries were 45 ^{o} and 85^o. The absorbing boundaries were placed 20 cells away from the cube surfaces. The time response of the E $_y$ field for two sets of coef ficients *a*

lines. The 12 transmission lines linking the Cartesian mesh of nodes together have the characteristic impedance of free space. Each line is associated with two f ields. For example, a voltage impulse incident upon the port 3 is associated with the field quantities E_y and H_z.

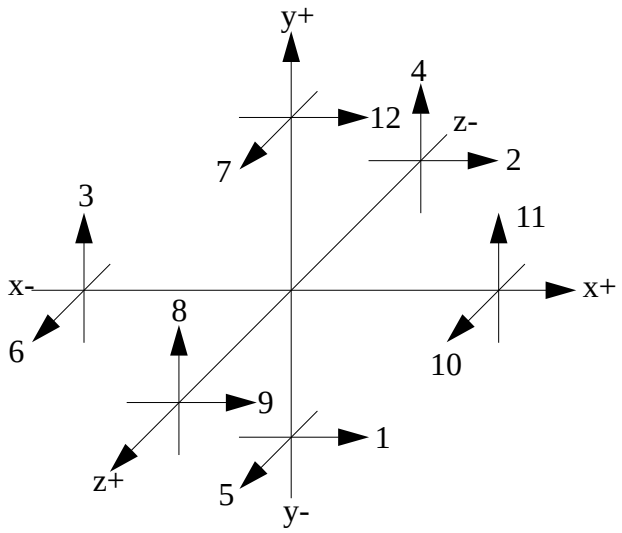

Fig. 1: The Symmetrical Condensed Node

2. ABSORBING BOUNDARY CONDITIONS

To obtain good absorption over a wide range of incident angles, we have concatenated two f irst-order Higdon's boundary operators to obtain a second-order absorbing boundary condition [9]. A voltage impulse reflected from the absorbing boundary can be computed from the knowledge of impulses in the cells in front of the boundary using the following equation:

$$\begin{aligned} = {} & (\alpha_1+\alpha_2)\,V^{n-1}(m,j,k) - \alpha_1\alpha_2 V^{n-2}(m,j,k) + (\beta_1+\beta_2)\,V^{n}(m-1,j,k) \\ & + (\gamma_1+\gamma_2-\alpha_1\beta_2-\beta_1\alpha_2)\,V^{n-1}(m-1,j,k) - (\alpha_1\gamma_2+\gamma_1\alpha_2)\,V^{n-2}(m-1,j,k) \\ & -\beta_1\beta_2 V^{n}(m-2,j,k) - (\beta_1\gamma_2+\gamma_1\beta_2)\,V^{n-1}(m-2,j,k) - \gamma_1\gamma_2 V^{n-2}(m-2,j,k) \end{aligned} \quad (1)$$

The interpolation coefficients are:

$$\alpha_i = \frac{(a-g_i(1-b))}{(a-1-g_i(1-b)-\varepsilon_i\Delta l)}, \beta_i = \frac{(a-1+g_i b)}{(a-1-g_i(1-b)-\varepsilon_i\Delta l)}, \gamma_i = \frac{(-a-bg_i)}{(a-1-g_i(1-b)-\varepsilon_i\Delta l)} \quad (2)$$

where coefficients *a* and *b* are weighted time and space averages of the space and time differences, respectively. ε_1 and ε_2 are damping factors. The parameter g_i is

$$= \frac{\cos\theta_i}{c} \quad \frac{\Delta l}{\Delta t} \quad (3)$$

where Δl and Δt are the space resolution and time step respectively . θ_i are the incidence angles. For the symmetrical condensed node, g_i becomes = $\cos\theta_i$.

RCS OF HIGH PERMITTIVITY CUBES COMPUTED WITH THE TLM METHOD

Channabasappa Eswarappa and Wolfgang J. R. Hoefer

NSERC/MPR Teltech Research Chair in RF Engineering, Department of Electrical and Computer Engineering, University of Victoria, Victoria, B.C., CANADA V8W 3P6

ABSTRACT

In this paper, the three-dimensional time domain Transmission Line Matrix (TLM) method has been applied to compute the RCS of dielectric cubes of relative permittivity 37.84 and 79.46, and comparison has been made with published measurements [1]. Since the high permittivity cubes ring for a very long time, very good quality absorbing boundary conditions having long term stability are required. We have achieved these by modifying Higdon's absorbing boundary conditions. Long term stability has been obtained by using proper discretization of the boundary operators (derivatives), and very low reflections have been obtained by concatenating two first-order boundary operators. We have obtained stability beyond 60,000 time steps by placing the absorbing boundaries just 20 cells away from the cube surfaces (cube size is 15 cells). The RCS data computed with the TLM method agree very well with the measurements published in [1]. The frequency shift between the TLM results and the measurements is negligible, while a considerable frequency shift has been reported between results obtained with FDTD and measurement [1].

1. INTRODUCTION

The Transmission Line Matrix (TLM) method is a numerical technique in which both space and time are discretized [2]. The simulation of propagation of electromagnetic waves is done through scattering of impulses in a 3-D meshed network of transmission lines. This method is suitable for computation of radar cross-section (RCS) of complex bodies. The RCS over a wide frequency bandwidth can be obtained from a single TLM simulation. Earlier studies on computation of RCS using the TLM method have concentrated mainly on perfectly conducting targets [3-6]. This paper studies the scattering properties of high permittivity dielectric cubes. As these cubes ring for a very long time, highly stable absorbing boundary conditions are required for a TLM analysis as compared to the perfectly conducting targets. Eventhough a number of absorbing boundary conditions have been reported in the literature, Higdon's absorbing boundary conditions [7] have been found to perform better than others [8]. The absorption properties in the required frequency range can be optimized by taking advantage of the prior information about the incident angles and by combining several first-order boundary operators [9-10]. Also, the long term stability can be obtained by choosing the proper finite differences for the boundary operators.

We have used the symmetrical condensed node (SCN) TLM [11] (shown in Fig.1) for obtaining the scattered tangential electric and magnetic fields on the fictitious current surfaces. The advantages of this node when compared to the expanded TLM node and Yee's FDTD node are the following: boundary description is easier, and all six field components can be defined at single points in space. It has six branches, each branch consisting of two uncoupled two-wire transmission